# Measurement of the pion form factor for $M^2_{\pi\pi}$ between 0.1 and 0.85 GeV$^2$ with the KLOE detector

KLOE collaboration*

presented by Stefan E. Müller 1)

1 Institut für Kernphysik, Johannes Gutenberg-Universität, Johann-Joachim-Becher-Weg 45, 55128 Mainz, Germany



**Abstract** The KLOE experiment at the $\phi$-factory DA$\Phi$NE has measured the pion form factor in the range between $0.1 < M^2_{\pi\pi} < 0.85$ GeV$^2$ using events taken at $\sqrt{s} = 1$ GeV with a photon emitted at large polar angles in the initial state. This measurement extends the $M^2_{\pi\pi}$ region covered by KLOE ISR measurements of the pion form factor down to the two pion production threshold. The value obtained in this measurement of the dipion contribution to the muon anomalous magnetic moment of $\Delta a_\mu^{\pi\pi} = (478.5 \pm 2.0_{\rm stat} \pm 4.8_{\rm syst} \pm 2.9_{\rm theo}) \cdot 10^{-10}$ further confirms the discrepancy between the Standard Model evaluation for $a_\mu$ and the experimental value measured by the (g-2) collaboration at BNL.

**Key words** Hadronic cross section, initial state radiation, pion form factor, muon anomaly

**PACS** 13.40.Gp, 13.60.Hb, 13.66.Bc, 13.66.Jn

## 1 Introduction

The anomalous magnetic moment of the muon, $a_\mu$, is one of the best known quantities in particle physics. Recent theoretical evaluations [1, 2, 3] find a discrepancy of 3 - 4 standard deviations from the value obtained from the g-2 experiment at Brookhaven [4, 5]. A large part of the uncertainty on the theoretical estimates comes from the leading order hadronic contribution $a_\mu^{\rm had,lo}$, which at low energies is not calculable by perturbative QCD, but has to be evaluated with a dispersion integral using measured hadronic cross sections. The use of initial state radiation (ISR) has opened a new way to obtain these cross sections at particle factories operating at fixed energies [6]. The region below 1 GeV, which is accessible with the KLOE experiment in Frascati, is dominated by the $\pi^+\pi^-$ final state and contributes with $\sim 70\%$ to $a_\mu^{\rm had,lo}$, and $\sim 60\%$ to its uncertainty. Therefore, improved precision in the $\pi\pi$ cross section would result in a reduction of the uncertainty on the leading order hadronic contribution to $a_\mu$, and in turn improve the Standard Model prediction for $a_\mu$.

## 2 Measurement of $\sigma_{\pi\pi}$

The measurement has been performed with the KLOE detector at the DA$\Phi$NE $e^+e^-$ collider in Frascati. DA$\Phi$NE is a $\phi$-factory that usually operates at $\sqrt{s} \simeq M_\phi$, and has delivered ca. 2.5 fb$^{-1}$ of data to the KLOE experiment up to the year 2006, from which KLOE has reported two measurements of the $\pi\pi$ cross section between 0.35 and 0.95 GeV$^2$ [7, 8]. In addition, about 250 pb$^{-1}$ of data have been collected at $\sqrt{s} \simeq 1$ GeV, 20 MeV below the $\phi$ resonance, from which the new results were obtained. Running below the $\phi$ resonance diminishes the backgrounds from the copious $\phi$ decay products, including scalar mesons. As DA$\Phi$NE was designed to operate at a fixed energy around $M_\phi$, the differential cross section $\mathrm{d}\sigma(e^+e^- \to \pi^+\pi^- + \gamma_{\rm ISR})/\mathrm{d}M^2_{\pi\pi}$ is measured, and the total cross section $\sigma_{\pi\pi} \equiv \sigma_{e^+e^- \to \pi^+\pi^-}$ is evaluated using the formula [11]:

$$s \cdot \frac{\mathrm{d}\sigma_{\pi\pi\gamma_{\rm ISR}}}{\mathrm{d}M^2_{\pi\pi}} = \sigma_{\pi\pi}(M^2_{\pi\pi})\ H(M^2_{\pi\pi}, s)\ , \qquad (1)$$

in which $s$ is the squared $e^+e^-$ center of mass energy, and $H$ is a radiator function obtained from theory de-

* F. Ambrosino, A. Antonelli, M. Antonelli, F. Archilli, P. Beltrame, G. Bencivenni, C. Bini, C. Bloise, S. Bocchetta, F. Bossi, P. Branchini, G. Capon, T. Capussela, F. Ceradini, P. Ciambrone, E. De Lucia, A. De Santis, P. De Simone, G. De Zorzi, A. Denig, A. Di Domenico, C. Di Donato, B. Di Micco, M. Dreucci, G. Felici, S. Fiore, P. Franzini, C. Gatti, P. Gauzzi, S. Giovannella, E. Graziani, M. Jacewicz, W. Kluge, J. Lee-Franzini, M. Martini, P. Massarotti, S. Meola, S. Miscetti, M. Moulson, S. Müller, F. Murtas, M. Napolitano, F. Nguyen, M. Palutan, A. Passeri, V. Patera, P. Santangelo, B. Sciascia, T. Spadaro, L. Tortora, P. Valente, G. Venanzoni, R. Versaci, G. Xu

1) E-mail: muellers@kph.uni-mainz.de

scribing the photon emission in the initial state. Final State Radiation (FSR) terms are neglected in Eq. 1, but are taken into account properly in the analysis.

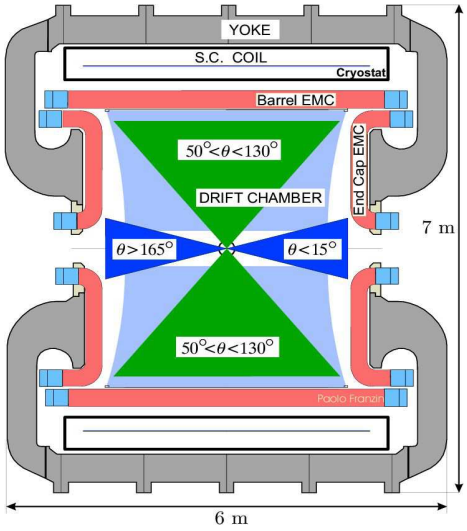


Fig. 1. Schematic view of the KLOE detector with selection regions.

The KLOE detector (Fig. 1) consists of a high resolution drift chamber ($\sigma_p/p \leq 0.4\%$) [9] and an electromagnetic calorimeter with excellent time ($\sigma_t \sim 54$ ps$/\sqrt{E\ [\mathrm{GeV}]} \oplus 100$ ps) and good energy ($\sigma_E/E \sim 5.7\%/\sqrt{E\ [\mathrm{GeV}]}$) resolution [10].

### 2.1 Event selection

The previous KLOE analyses [7, 8] used selection cuts in which photons are emitted within a cone of $\theta_\gamma < 15°$ around the beamline (narrow cones in Fig. 1) and the two charged pion tracks have $50° < \theta_\pi < 130°$ (wide cones in Fig. 1). In this configuration, the photon is not explicitly detected, its direction is reconstructed from the tracks' momenta by closing kinematics: $\vec{p}_\gamma \simeq \vec{p}_{\mathrm{miss}} = -(\vec{p}_{\pi^+} + \vec{p}_{\pi^-})$. While these cuts guarantee a high statistics for ISR signal events, and a reduced contamination from the resonant process $e^+e^- \to \phi \to \pi^+\pi^-\pi^0$ in which the $\pi^0$ mimics the missing momentum of the photon(s) and from the final state radiation process $e^+e^- \to \pi^+\pi^-\gamma_{\mathrm{FSR}}$, a highly energetic photon emitted at small angle forces the pions also to be at small angles (and thus outside the selection cuts), resulting in a kinematical suppression of events with $M^2_{\pi\pi} < 0.35$ GeV$^2$. To access the two pion threshold, a new analysis is performed requiring events that are selected to have a photon at large polar angles between $50° < \theta_\gamma < 130°$ (wide cones in Fig. 1), in the same angular region as the pions to be included. The drawback using such acceptance cuts is a reduction in statistics of about a factor 5, as well as an increase of events with final state radiation and from $\phi$ radiative decays compared to the small angle photon acceptance criterion. The uncertainty on the model dependence of the $\phi$ radiative decays to the scalars $f_0(980)$ and $f_0(600)$ together with $\phi \to \rho\pi \to (\pi\gamma)\pi$ has a strong impact on the measurement [12]. As an obvious way out of this dilemma, the present analysis uses the data taken by the KLOE experiment in 2006 at a value of $\sqrt{s} = 1$ GeV, about 5 $\Gamma_\phi$ outside the narrow peak of the $\phi$ resonance ($\Gamma_\phi = 4.26 \pm 0.04$ MeV [13]). This reduces the effect due to contributions from $f_0\gamma$ and $\varrho\pi$ decays of the $\phi$-meson to within $\pm 1\%$.

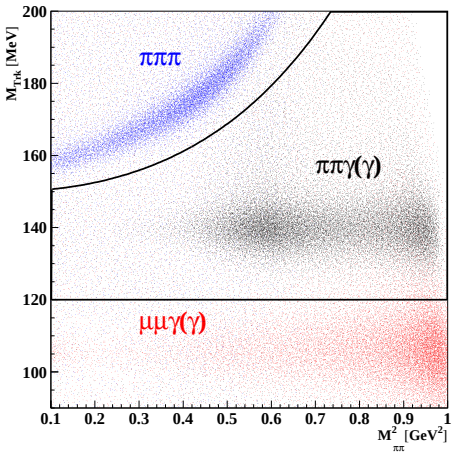


Fig. 2. MC simulation of $M_{\mathrm{trk}}$ vs. $M^2_{\pi\pi}$. $\pi^+\pi^-\gamma$ and $\mu^+\mu^-\gamma$ events are located around $m_\pi$ and $m_\mu$ respectively, while $\pi^+\pi^-\pi^0$ events occupy a region in the upper left of the plot. The black lines represent the cuts used in the analysis.

Contaminations from the processes $\phi \to \pi^+\pi^-\pi^0$ and $e^+e^- \to \mu^+\mu^-\gamma$ are rejected by cuts in the kinematical variables *trackmass** and $\Omega^\dagger$ (see Fig. 2 and Fig. 3). A particle ID estimator based on calorimeter information and time-of-flight is used to efficiently suppress the high rate of radiative Bhabhas. The radiative differential cross section is then obtained subtracting the residual background events, $N_{bkg}$, dividing by the selection efficiencies, $\varepsilon_{sel}(M^2_{\pi\pi})$, and the integrated luminosity using the formula

$$\frac{\mathrm{d}\,\sigma_{\pi\pi\gamma}}{\mathrm{d}\,M^2_{\pi\pi}} = \frac{N_{obs} - N_{bkg}}{\Delta M^2_{\pi\pi}} \frac{1}{\varepsilon_{sel}(M^2_{\pi\pi})\ \mathcal{L}}\ , \qquad (2)$$

*The trackmass is defined using conservation of 4-momentum under the hypothesis that the final state consists of two charged particles with equal mass $M_{\mathrm{trk}}$ and one photon.

$^\dagger\Omega$ is the three-dimensional angle between the direction of the selected photon and the missing momentum.

where the observed events are selected in bins of $\Delta M^2_{\pi\pi} = 0.01$ GeV$^2$. The residual background content is found by fitting the $M_{trk}$ spectrum of the selected data sample with a superposition of Monte Carlo distributions describing the signal and background sources. The fit parameters are the fractional normalization factors for these Monte Carlo distributions, obtained in intervals of $M^2_{\pi\pi}$.

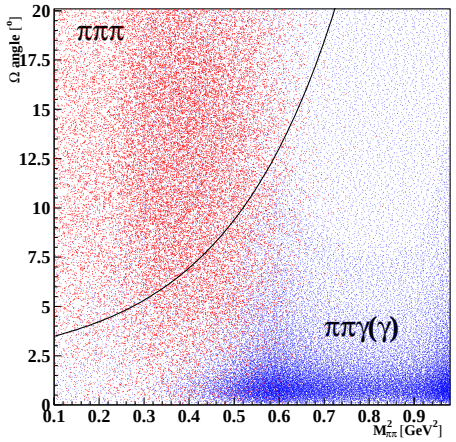


Fig. 3. MC simulation of Ω-angle vs. $M^2_{\pi\pi}$. $\pi^+\pi^-\gamma$-events (blue) are distributed at small values of Ω, while the $\pi^+\pi^-\pi^0$ events (red) occupy the region below 0.5 GeV$^2$ at larger values of Ω. The black line represents the cut used in the analysis.

### 2.2 Luminosity

The absolute normalization of the data sample is performed by measuring Bhabha events at large angles ($55° < \theta < 125°$), with an effective cross section of $\sigma_{\rm Bhabha} \simeq 430$ nb. To obtain the integrated luminosity, $\mathcal{L}$, the observed number of Bhabha events is divided by the effective cross section evaluated by the Monte Carlo generator `Babayaga@NLO` [14, 15], which includes QED radiative corrections with the parton shower algorithm, and which has been interfaced with the KLOE detector simulation. A detailed description of the KLOE luminosity measurement can be found in [16].

### 2.3 Radiative corrections

The radiator function $H$ used to get $\sigma_{\pi\pi}$ in Eq. 1 is obtained from the `PHOKHARA` Monte Carlo generator, which calculates the complete next-to-leading order ISR effects [17]. In addition, the cross section is corrected for the vacuum polarisation [18] (running of $\alpha_{em}$), and the shift between the measured value of $M^2_{\pi\pi}$ and the squared virtual photon mass $M^2_{\gamma^*} \equiv (M^0_{\pi\pi})^2$ for events with photons from final state radiation. Again the `PHOKHARA` generator, which includes FSR effects in the pointlike-pions approximation, is used to estimate the latter [19], and a matrix relating $M^2_{\pi\pi}$ to $M^2_{\gamma^*}$ by giving the probability for an event in a bin of $M^2_{\pi\pi}$ to end up in a bin of $M^2_{\gamma^*}$ is used to correct the spectrum.

### 2.4 Results

Using Eq. 1 and Eq. 2, one obtains the two-pion cross section $\sigma_{\pi\pi}$. The squared modulus of the pion form factor $|F_\pi|^2$ can then be derived using the relation‡

$$|F_\pi(s')|^2 = \frac{3}{\pi}\frac{s'}{\alpha^2_{\rm em}\beta^3_\pi}\sigma_{\pi\pi}(s') \ , \qquad (3)$$

where $s' = (M^0_{\pi\pi})^2$ is the squared momentum transferred by the virtual photon and $\beta_\pi = \sqrt{1-\frac{4m^2_\pi}{s'}}$ is the pion velocity.

Fig. 4 shows $|F_\pi|^2$ as a function of $(M^0_{\pi\pi})^2$ for the new KLOE09 measurement and the previous KLOE publication, KLOE08. As can be seen from Fig. 5, both measurements are in very good agreement, especially above 0.5 GeV$^2$.

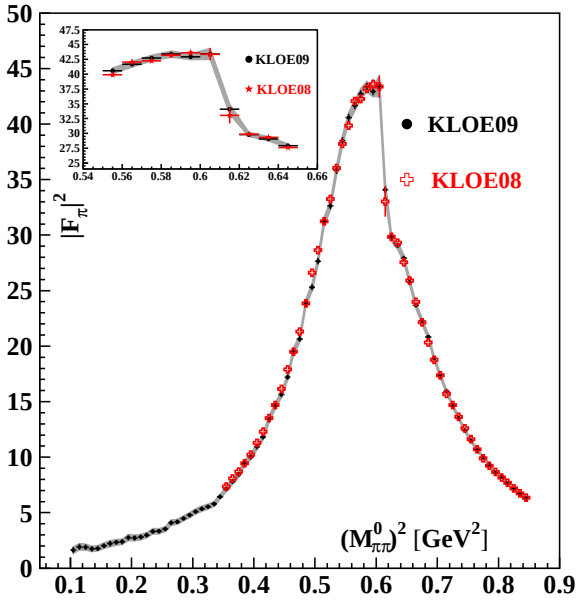


Fig. 4. Pion form factor $|F^2_\pi|$ obtained in the present (KLOE09) and the previous (KLOE08) analysis. KLOE09 data points have statistical error attached, the grey band gives the statistical and systematic uncertainty (added in quadrature). Errors on KLOE08 points contain the combined statistical and systematic uncertainty.

‡In addition, the choice of radiative corrections applied to $\sigma_{\pi\pi}$ and $|F_\pi|^2$ may differ betwen the two. We adopt the definition used in [22, 23, 24], in which $\sigma_{\pi\pi}$ is inclusive with respect to final state radiation, and undressed from vacuum polarisation effects; while $|F_\pi|^2$ contains vacuum polarisation effects and final state radiation is removed.

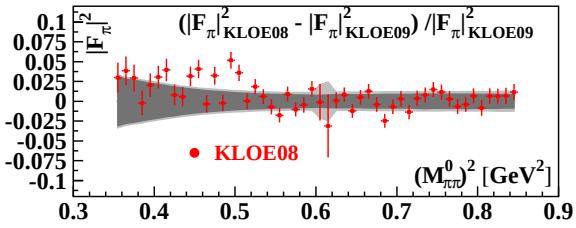


Fig. 5. Fractional difference between $|F_\pi^2|$ from the KLOE08 and the KLOE09 analysis. The band in dark grey represents the statistical error of the KLOE09 result, the band in lighter grey gives the statistical and systematic uncertainty (added in quadrature) for the KLOE09 result. Errors on KLOE08 points contain the combined statistical and systematic uncertainty.

The cross section corrected for the running of $\alpha_{em}$ and inclusive of FSR, $\sigma^{bare}_{\pi\pi(\gamma)}$, is used to determine $\Delta a_\mu^{\pi\pi}$ via a dispersion integral:

$$a_\mu^{\pi\pi} = \frac{1}{4\pi^3}\int_{s_{min}}^{s_{max}} \mathrm{d}s'\ \sigma^{bare}_{\pi\pi(\gamma)}(s')\,K(s')\ , \qquad (4)$$

where the lower and upper bounds are $s_{min} = 0.10$ GeV$^2$ and $s_{max} = 0.85$ GeV$^2$ in the present analysis, and the kernel function $K(s)$ is described in [21]. We obtain a value of

$$\Delta a_\mu^{\pi\pi}(0.1-0.85\,\mathrm{GeV}^2) = (478.5 \pm 2.0_{\rm stat} \pm 4.8_{\rm exp} \pm 2.9_{\rm theo}) \cdot 10^{-10}. \qquad (5)$$

| | |
|---|---|
| Reconstruction Filter | negligible |
| Background subtraction | 0.5 % |
| $f_0 + \rho\pi$ bkg. | 0.4 % |
| $\Omega$ cut | 0.2 % |
| Trackmass cut | 0.5 % |
| $\pi$/e-ID | negligible |
| Tracking | 0.3 % |
| Trigger | 0.2 % |
| Acceptance | 0.4 % |
| Unfolding | negligible |
| Software Trigger (L3) | 0.1 % |
| Luminosity $(0.1_{th} \oplus 0.3_{exp})\%$ | 0.3 % |
| Total exp. systematics | 1.0 % |
| FSR resummation | 0.3 % |
| Vacuum Polarization | 0.1 % |
| Rad. function $H$ | 0.5 % |
| Total theory systematics | 0.6 % |

Table 1. List of systematic errors on the $\Delta a_\mu^{\pi\pi}$ evaluation.

The evaluation of $\Delta a_\mu^{\pi\pi}$ in the range between 0.35 and 0.85 GeV$^2$ allows to compare the result obtained in this new analysis with the previously published result by KLOE [8]:

| KLOE Analysis | $\Delta a_\mu^{\pi\pi}(0.35-0.85\,\mathrm{GeV}^2)\times 10^{-10}$ |
|---|---|
| KLOE09 | $376.6 \pm 0.9_{\rm stat} \pm 2.4_{\rm exp} \pm 2.1_{\rm theo}$ |
| KLOE08 | $379.6 \pm 0.4_{\rm stat} \pm 2.4_{\rm exp} \pm 2.2_{\rm theo}$ |

The two values are in good agreement.

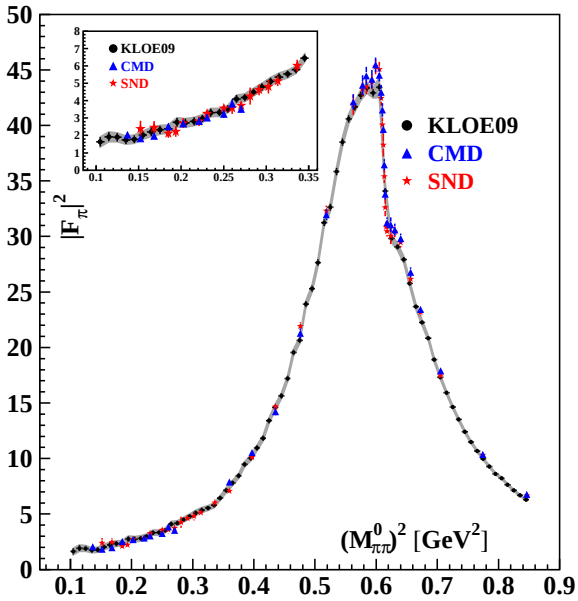


Fig. 6. Pion form factor $|F_\pi^2|$ obtained in the present analysis (KLOE09) and results from the CMD and SND experiments. KLOE09 data points have statistical error attached, the grey band gives the statistical and systematic uncertainty (added in quadrature). Errors on CMD2 and SND points contain the combined statistical and systematic uncertainty.

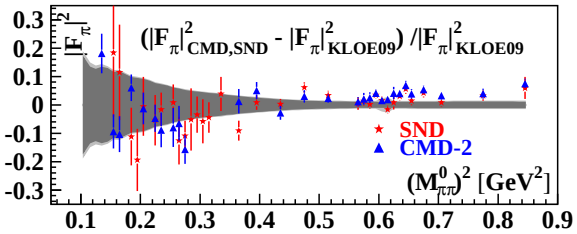


Fig. 7. Fractional difference between $|F_\pi^2|$ from KLOE09 and the CMD and SND experiments. The band in dark grey represents the statistical error of the KLOE09 result, the band in lighter grey gives the statistical and systematic uncertainty (added in quadrature) for the KLOE09 result. Errors on CMD and SND points contain the combined statistical and systematic uncertainty.

### 2.5 Comparison with other experiments

Fig. 6 and Fig. 7 show the KLOE09 result for $|F_\pi|^2$ together with results from the CMD-2 [22, 23] and SND [24] experiments in Novosibirsk. While on the $\rho$-peak and above, the new result confirms the KLOE08 result being lower than the Novosibirsk results, below the $\rho$-peak the three experiments show good agreement.

## 3 Forward-backward asymmetry

The interference in the amplitudes for ISR and FSR is odd under the exchange $\pi^+ \leftrightarrow \pi^-$. This gives rise to a non-vanishing asymmetry of the distributions in the polar angle $\theta$ for the pions [11]. A common way to express this is the *forward-backward* asymmetry $\mathcal{A}_{\rm FB}$:

$$\mathcal{A}_{\rm FB}(M^2_{\pi\pi}) = \frac{N_{\pi^+}(\theta > 90^\circ) - N_{\pi^+}(\theta < 90^\circ)}{N_{\pi^+}(\theta > 90^\circ) + N_{\pi^+}(\theta < 90^\circ)}. \quad (6)$$

This quantity is an ideal tool to test the validity of models used in Monte Carlo to describe the pionic final state radiation. In a similar way, radiative decays of the $\phi$ meson into scalars decaying into $\pi^+\pi^-$ contribute to the asymmetry [19, 20]. As can be seen in Fig. 8 and Fig. 9, this has a large effect on the asymmetry going from data taken at $\sqrt{s} \simeq 1$ GeV to data taken at $\sqrt{s} = M_\phi$, especially in the energy region below the $\rho$-meson mass. Outside the $\phi$-resonance, the asymmetry is almost completely dominated by the pionic final state radiation, while on the peak of the resonance, the decays of the $\phi$-meson to $f_0\gamma$ and also $\rho\pi$ contribute significantly. A comparison with a Monte Carlo prediction using the PHOKHARA event generator [25] with a model for $\phi$-decays and parameters from [26], together with a pointlike-pion description for the pionic final state radiation, shows a good agreement with the data for both sets of data. Qualitatively, the theoretical descriptions used to model the different contributions in the simulation agree well with the data, although at low $M^2_{\pi\pi}$ the data statistics becomes poor and the data asymmetry points have large errors. In particular, the *off-peak* data in Fig. 8 shows very good agreement above 0.35 GeV$^2$ with the pointlike-pion description for FSR. Further work is in progress to determine the impact of different models for FSR on the asymmetry, as well as to estimate higher order effects [27]. In future, the larger dataset from 2004-2005, which is almost 10 times larger than the data shown in Fig. 9, may be used to determine with high precision the parameters of the $\phi$ decay contributions, in combination with the results from the neutral channel $\phi \to \pi^0\pi^0\gamma$ and the assumption of isospin symmetry. This will then in turn allow to perform a precise *on-peak* measurement of the pion form factor down to the production threshold, using the full data sample of about 2 fb$^{-1}$ accumulated by the KLOE experiment.

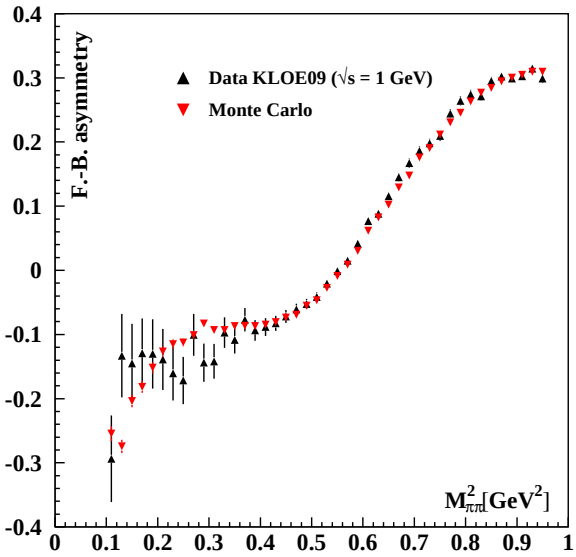


Fig. 8. Preliminary forward-backward asymmetry for KLOE09 data taken at $\sqrt{s} \simeq 1$ GeV, and the corresponding Monte Carlo prediction using the PHOKHARA event generator with model and parameters from [26].

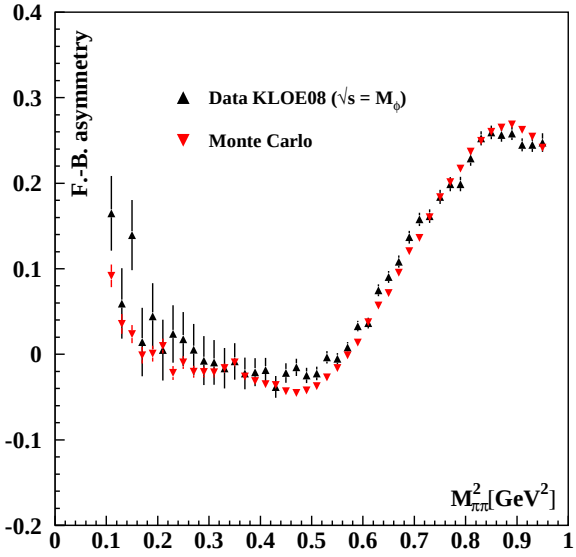


Fig. 9. Preliminary forward-backward asymmetry for KLOE08 data taken at $\sqrt{s} = M_\phi$, and the corresponding Monte Carlo prediction using the PHOKHARA event generator with model and parameters from [26].

## 4 Conclusions and outlook

The KLOE experiment has performed a new measurement of the pion form factor $|F_\pi|^2$ in the $M^2_{\pi\pi}$ range between 0.1 and 0.85 GeV$^2$. The result is in very good agreement with the previous KLOE result, and extends it down to the two-pion threshold. Reasonable agreement was found (especially at low energies) with the results obtained from the Novosibirsk experiments CMD-2 and SND. The new KLOE result further confirms the discrepancy between the Standard Model evaluation for $a_\mu$ and the experimental value measured by the (g-2) collaboration at BNL.

A next step at KLOE will be the measurement of the pion form factor using a normalization to radiative muon events in each bin. In this way, many theoretical uncertainties would become negligible, since the radiator function, the vacuum polarisation and the absolute luminosity would cancel out in the ratio of $\pi\pi\gamma$ over $\mu\mu\gamma$ events to first order. Pions and muons are separated and identified using kinematical variables (e.g. the aforementioned trackmass variable) [28]. The analysis is in a very advanced state and a systematic precision similar to the one obtained in the absolute measurement is expected.

The forward-backward asymmetry $\mathcal{A}_{\rm FB}$ is an important tool to test models for pionic final state radiation and radiative decays of the $\phi$ mesons to scalars. A good check on the validity of models and their parameters is crucial for precise measurements of the pion form factor below 1 GeV using initial state radiation, especially when running at the energy of $\sqrt{s} = M_\phi$.

### References


1 F. Jegerlehner and A. Nyffeler, Phys. Rept. **477** (2009) 1
2 T. Teubner, these proceedings
3 M. Davier, these proceedings
4 G. W. Bennett *et al.* [Muon g-2 Coll.], Phys. Rev. D **73** (2006) 072003
5 B. L. Roberts, these proceedings
6 S. Actis *et al.*, arXiv:0912.0749 [hep-ph]
7 A. Aloisio *et al.* [KLOE Coll.], Phys. Lett. B **606** (2005) 12
8 F. Ambrosino *et al.* [KLOE Coll.], Phys. Lett. B **670**, 285 (2009)
9 M. Adinolfi *et al.*, Nucl. Inst. Meth. A **488**, 51 (2002)
10 M. Adinolfi *et al.*, Nucl. Inst. Meth. A **482**, 364 (2002)
11 S. Binner, J. H. Kühn and K. Melnikov, Phys. Lett. B **459**, 279 (1999)
12 D. Leone, PhD thesis, KA-IEKP-2007-7 (2007)
13 C. Amsler *et al.* [Particle Data Group], Phys. Lett. B **667**, 1 (2008)
14 C. M. Carloni Calame *et al.*, Nucl. Phys. B **584**, 459 (2000)
15 G. Balossini *et al.*, Nucl. Phys. B **758**, 227 (2006)
16 F. Ambrosino *et al.* [KLOE Coll.], Eur. Phys. J. C **47**, 589 (2006)
17 H. Czyż, A. Grzelińska, J. Kühn, G. Rodrigo, Eur. Phys. J. C **27**, 563 (2003)
18 F. Jegerlehner, Nucl. Phys. Proc. Suppl. **162**, 22 (2006)
19 H. Czyż, A. Grzelińska, J. Kühn, Phys. Lett. B **611**, 116 (2005)
20 K. Melnikov, F. Nguyen, B. Valeriani, G. Venanzoni, *Phys. Lett. B* **477**, 114 (2000)
21 S. J. Brodsky, E. De Rafael, Phys. Rev. **168**, 1620 (1967)
22 R. R. Akhmetshin et al. [CMD-2 Coll.], *Phys. Lett. B* **648**, 28 (2007)
23 R. R. Akhmetshin et al. [CMD-2 Coll.], *JETP Lett.* **84**, 413 (2006)
24 M. N. Achasov et al. [SND Coll.], *J. Exp. Theor. Phys.* **103**, 380 (2006)
25 O. Shekhovtsova, PHOKHARA6.1 (`http://ific.uv.es/~rodrigo/phokhara/`), unpublished
26 F. Ambrosino *et al.* [KLOE Coll.], Eur. Phys. J. C **49**, 473 (2007)
27 S. Ivashyn, H. Czyż, A. Korchin, arXiv:0910.5335 (2009)
28 S. E. Müller, F. Nguyen, Nucl. Phys. Proc. Suppl. **162**, 90 (2004)